AN EXPERIMENTAL ANALYSIS OF THE STABILITY AND THE DYNAMICS OF AXISYMMETRIC LIQUID BRIDGES BETWEEN UNEQUAL DISKS

J. MESEGUER, P. RODRÍGUEZ DE FRANCISCO
Laboratorio de Aerodinámica, E.T.S.I. Aeronáuticos, Universidad Politécnica de Madrid, 28040 Madrid, Spain
A. ISIDORO, E. FERNÁNDEZ, A. CARRETERO
Instituto Nacional de Técnica Aeroespacial (INTA), 28850 Torrejón de Ardoz, Spain

Abstract—In this paper, experimental results related to both the stability and the dynamics of axisymmetric liquid bridges between unequal disks are presented. Experiments have been performed by using a drop tower facility and the response of the liquid bridge to a sudden change of the acceleration level acting on it has been obtained. Concerning stability limits, experimental results are in agreement with theoretical ones; the agreement between theoretical and experimental results being worse when the breaking of the liquid column is considered; available numerical results obtained through an one-dimensional model for the liquid bridge dynamics give breaking times which are almost half the breaking times measured in experiments.

INTRODUCTION

The fluid configuration considered in this paper consists of an isothermal, axisymmetric column of liquid of volume V, held by surface tension forces between two coaxial, parallel, solid disks placed a distance L apart, as sketched in Fig. 1. The liquid is subjected to a microgravity field, g, acting parallel to the liquid column axis. Such fluid configuration, known as liquid bridge, can be uniquely defined by the following dimensionless parameters: the ratio of the smaller disk radius, R_1, to the large one, R_2, $K = R_1/R_2$, the slenderness $\Lambda = L/(2R_0)$, where $R_0 = (R_1 + R_2)/2$, the dimensionless volume $V = V/(\pi R_0^2 L)$ and the Bond number $B = \Delta\rho g R_0^2/\sigma$, where $\Delta\rho$ stands for the difference between the density of the liquid of the column and the density of the surrounding medium, and σ stands for the surface tension.

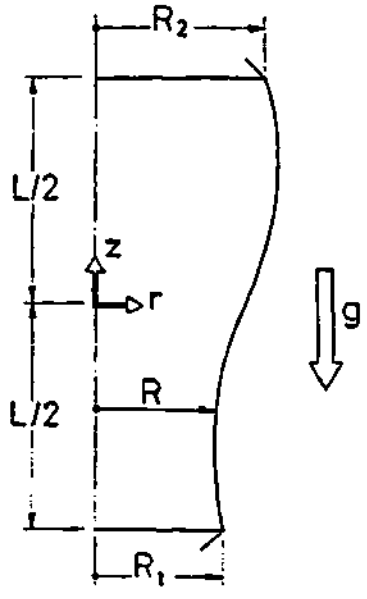

Fig. 1. Geometry and coordinate system for the liquid bridge problem.

The stability of liquid bridges has attracted the attention of many investigators during the last two decades. In early studies only liquid bridges between equal disks, $K = 1$, and in gravitationless conditions, $B = 0$, were considered. It was found that for each value of the slenderness there is a minimum volume of liquid for which the liquid bridge is stable [1, 2]; liquid bridges having less volume, or higher slenderness, than those corresponding to the minimum volume stability limit will break into two main drops (plus a small satellite droplet) whose volumes depend on the value of the slenderness Λ. It was demonstrated that effects like Bond number, $B \neq 0$, or unequal disks, $K \neq 1$, increase the minimum volume stability limit [3-5]: for a given slenderness the liquid bridge needs more volume of liquid to be stable when $B \neq 0$ than when $B = 0$, and the same happens with the relative size of the disks, for a given slenderness the stability limit is higher when $K \neq 1$ than in the case of equal disks ($K = 1$). The reason of this behaviour can be roughly explained taking into account that each one of these two effects are non-symmetric with respect to the middle plane parallel to the disks. Each one of these effects isolately considered force the appearance of a neck close to one of the disks which decreases the stability of the liquid column; in consequence, the volume of liquid must be increased, or the slenderness decreased, to compensate this necking destabilizing effect. However, when both effect are simultaneously considered the situation can be rather different. If both effects are in phase (both effects tend to cause a neck close to the same disk) the resulting configuration is less stable than when each one of the two effects are considered separately; but if both effects are in counter-phase the resulting configuration is more stable than that resulting from the action of only one of them (see Fig. 2). According to the above explanation, a liquid bridge between unequal disks can be stable when subjected to an axial acceleration (provided the acceleration has the appropriate sense) and become unstable in gravitationless conditions [6-7].

Besides stability studies, several attemps have been made to analyze the dynamics of liquid bridges. Concerning the breaking process, available theoreti

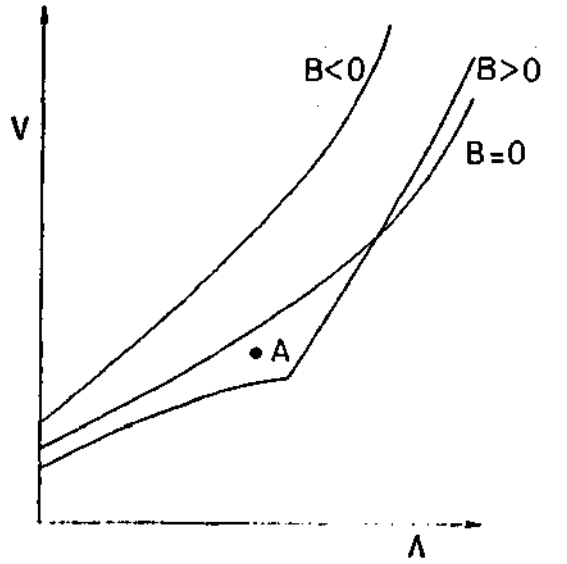

Fig. 2. Variation with the Bond number, B, of the stability limit of minimum volume of liquid bridges between unequal disks, $K \neq 1$. Each one of the curves splits the plane in two regions; points belonging to the region placed over the corresponding stability-limit curve represent stable configurations whereas those belonging to the lower region represent unstable configurations. Note that a point like A can be stable or unstable depending on the value of the Bond number.

cal results have been obtained by using a onedimensional model derived from capillary jet theory [8-10], although recently some results obtained by using a more refined model have been published [11].

Stability limits of liquid bridges have been experimentally studied either on Earth (by using very small samples [12] or neutral buoyancy, the so-called Plateau technique [4,7,13,14]) or on board space-platforms [15,16]. Concerning the dynamics, the situation is rather different; leaving apart experimental studies dealing with the oscillation of liquid bridges, available experimental results related to the breakage of liquid bridges are mainly concerned with the final result of the breaking process (i.e., the volume of the drops resulting after breaking [15,17,18]) and, as far as we know, no attempts have been made dealing with the breaking process itself. The reason for this lack of experimental results is that some characteristics of the breaking process, for instance, the breaking time or the time variation of the neck radius, are strongly influenced by initial conditions, which are extremely difficult to be controlled during experimentation. Fortunately, there are other characteristics of the breaking process which are almost independent of the initial conditions, this is the case of the volume of the drops resulting after breaking, which have been used to check the suitability of mathematical models to predics this aspect of the dynamics of liquid bridges.

There is, however, an experimental situation in which initial conditions can be accurately controlled. Let us assume a liquid bridge between unequal disks ($K \neq 1$) subjected to a positive Bond number ($B > 0$) and with the appropriate values of both the slenderness and the volume, in such a way that the liquid column be stable (such a liquid bridge could be represented by a point like the one labelled as A in the Λ–V stability diagram shown in Fig. 2). If the Bond number is now set to zero, the resulting configuration will be unstable, and it will break. Roughly speaking, the above paragraph describes the experimental procedure followed in the experiments reported in this paper: a liquid bridge between unequal disks was formed inside a Plateau cell and the density of the outer liquid was adjusted to have a stable liquid bridge. Then the apparatus was dropped out in a drop tower facility and the evolution during the free falling ($B \sim 0$) of the liquid bridge interface was recorded. For a given slenderness such evolutions can be of breaking, if the volume of the liquid column is smaller than that of the stability limit, or, on the other hand, an oscillatory motion can appear provided the liquid bridge volume is high enough. In this way, such experimental procedure allows the experimental determination of stability limits of liquid bridges between unequal disks ($K \neq 1$, $B = 0$) and allows one to get some conclusions on the stability margin (the minimum amount of energy which is needed to force the breaking of a stable liquid bridge). The stability limit corresponding to liquid bridges with $K = 0.805$ and $B = 0$ has been experimentally checked by following the above described method, experimental results being in agreement with theoretical ones. In addition, some conclusions concerning the dynamics of liquid bridges are presented: experimental results are compared with theoretical predictions obtained by using a one-dimensional model for the liquid bridge dynamics whose main characteristics have been published elsewhere [8-9].

APPARATUS AND EXPERIMENTAL TECHNIQUE

The equipment used in the experiments here described consists of a liquid bridge cell (Plateau Tank, PT) in which liquid bridges are formed plus a CCD camera, a commercial video recorder and the background illumination system, all of them mounted on a platform placed inside the drop-capsule (Fig. 3).

Fig. 3. Sketch of the experimental set-up. 1) Plateau Cell, 2) CCD camera, 3) video recorder, and 4) background illumination.

The PT is a tight box made of aluminum with two transparent faces. The test chamber is 0.04 m x 0.04 m x 0.06 m and contains the two disks which allow the formation of a liquid bridge between them. The lower disk is fixed, whereas the upper one can be displaced up and down by means of a calibrated screw. The rod supporting the upper disk is at the same time the piston of the syringe which acts as the working liquid reservoir. In this way, when the upper

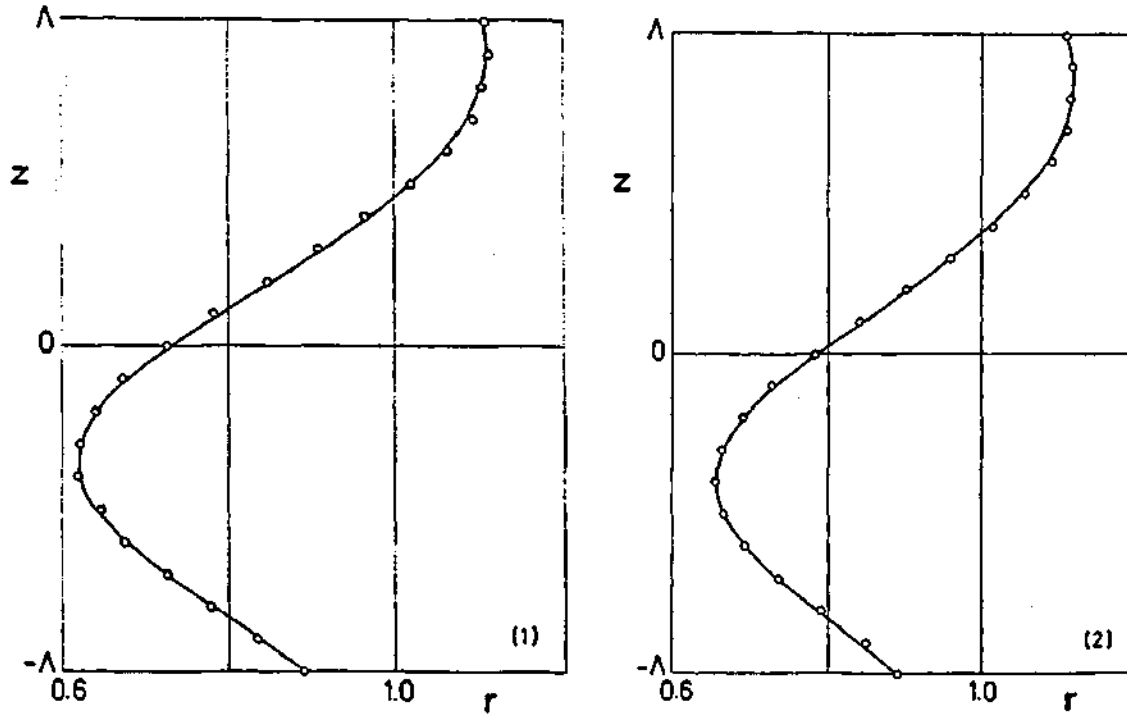

Fig. 4. Comparison between experimental (white circles) and theoretical (solid lines) interfaces of liquid bridges between unequal disks. $K = 0.805$. Solid lines indicate the best fitted theoretical interfaces. 1) $\Lambda = 2.19$, $V = 0.741$, $B = 0.024$; 2) $\Lambda = 2.30$, $V = 0.789$, $B = 0.023$.

disk is moved up the working liquid is forced to pass from the syringe to the liquid bridge through a duct which ends at a hole in the center of the upper disk. The contrary occurs when the upper disk is moved down: the liquid is forced to pass from the liquid bridge to the reservoir. To fill the reservoir, as well as to control the volume of liquid injected in the liquid bridge, the syringe has been provided with a quick-disconnect valve. There are other two quick-disconnect valves at the test chamber, which are used for the filling of the surrounding liquid (and the removal of the air trapped inside).

Working liquid was dimethyl silicone oil with a viscosity 20 times that of water and density $\varrho_w = 954$ kg.m^{-3}; outer bath was a mixture of methanol and water with the appropriate density to meet Bond number requirements. A typial value for the interface tension the liquid used is, according to the results reported in the literature [9,19], $\sigma = 0.017$ N.m^{-1}. These values of ϱ_w and σ, plus the value of the characteristic lenght, R_0, define the characteristic time of the experiments, $t_c = (\varrho_w R_0^3/\sigma)^{1/2}$. Experiments were performed at the drop tower facility existing at the Spanish National Institute for Aerospace Technics (INTA, Madrid) in which a free-falling time of 2 s is obtained; with this figure in mind the characteristic lenght $R_0 = 4.5 \times 10^{-3}$ m was chosen, so that the characteristic time becomes $t_c = 0.072$ s, which is some 30 times smaller than the free-fall time. The ratio of size of the disks was $K = 0.805$ and in all the experiments performed the liquid bridge configuration was similar to that represented in Fig. 1 (larger disk at the top).

Once a liquid bridge of the desired slenderness, volume and Bond number is formed (the slenderness can be accurately measured by reading the position of the micrometric screw, whereas volume and Bond number are measured from the images of the liquid bridge contour, as will be explained in the following) and the Plateau Tank fixed to the platform of the drop-capsule, the illumination and the image recording system are switched-on and, after a few seconds, the capsule is dropped out, so that the evolution of the liquid bridge interface is recorded during the free-falling period. The images of the liquid bridge before dropping are used to calculate the dimensionless volume of liquid (by integration of the liquid bridge contour) and the value of the Bond number, by fitting theoretical contours of the liquid bridge to experimental ones. The last procedure can be some what tedious because liquid bridge shapes must be numerically calculated and in the shape of a liquid bridge there is a large number of parameters involved [5,7]. In Fig. 4 some example of this fitting process are shown.

From the images recorded during the free-falling period the evolution of the whole liquid bridge interface can be analyzed. However, in the following the study has been restricted to the analysis of a characteristic section of the liquid bridge, this section being the one placed at one quarter of the lenght of the liquid column from the bottom disk (the smaller one). This section has been selected because it is close to the sections where the maximum deformation of the interface takes place if the liquid bridge either breaks or oscillates.

THEORETICAL BACKGROUND

Before presenting experimental results it would be convenient to give some basic ideas on the physics of the phenomenon under study. According to the experimental sequence described above, before free-falling there is a stable liquid bridge whose configuration is uniquely defined by the values of the set of parameters Λ,V,K,B. Then the liquid bridge is dropped, which means that, suddenly, the value of the Bond number is set to zero, the new set of parameters defining the fluid configuration during the falling period being $\Lambda,V,K,0$. Therefore, at $t=0$ the fluid configuration is a liquid bridge whose interface is not in equilibrium (once axial Bond number is removed) and, in consequence, a capillary pressure field appears which causes the movement of the liquid as well as the deformation of the interface. From now on there are two possibilities for this process initiated by a step change in the value of the Bond number. It could be that for the new set of values $(\Lambda,V,K,0)$ the liquid bridge be unstable; in such case the deformation of the interface will continue until the liquid column breakage takes place, the final configuration being two main drops, one drop anchored to the upper disk and the second to the lower one, plus a small satellite droplet. The second possibility is that the fluid configuration defined by $\Lambda,V,K,0$ lies in the stable region of the stability diagram. In this second case there are also other two possibilities for the evolution of the liquid bridge depending on both the initial energy of the liquid bridge and on how close to the stability limit the liquid bridge is. In order to simplify the explanation let us assume a liquid bridge surrounded by a medium of negligible density when compared with the density of the liquid bridge (this situation can be achieved by working with very small liquid bridges in an Earth laboratory or with large liquid columns in a space laboratory, an is rather different of the experimental conditions existing in a Plateau Tank, in which the liquid column is surrounded by another liquid of almost the same density). As already stated, at $t=0$ the interface is not equilibrium and the liquid bridge energy is higher than the one corresponding to the equilibrium shape. Such an excess of energy will force the evolution of the liquid bridge in such a way that, if no dissipative effects are accounted for, the total energy (surface energy plus kinetic one) will be kept constant; during the evolution there is a transfer from surface energy to kinetic one and viceversa. If the initial excess of energy (with respect to that of the stable equilibrium shape) is not too high the liquid bridge will oscillate with its natural frequency around the equilibrium shape (Fig. 5), the amplitude of the interface oscillation increasing as the excess of initial energy grows. However, if the initial excess of energy is high enough, the deformation of the interface during the evolution can be so high that forces the development of capillary instability. In this last case, once capillary instability has been triggered, the deformation of the interface will continue until the breaking of the liquid column occurs. After this reasoning it is clear that there is, for each stable liquid bridge, a stability margin whose magnitude can be measured by the difference, ΔE, between the energies of the stable configuration and the closer unstable one, as sketched in Fig. 5.

To illustrate the above reasoning, in Fig. 6 the variation with the dimensionless time of the non-dimensional surface energy (which has been made dimensionless with σR_0^2) of a liquid bridge with $\Lambda=2.85$, $V=1.3$, $K=0.805$ and $B=0$ is shown. The different curves correspond to different initial conditions (at $t=0$ the interface of the liquid bridge is that of a liquid column with the same Λ, V and K, but subjected to an axial Bond number $B_i\neq 0$). These results have been obtained by using a non-linear one-dimensional inviscid slice (ODIS) model for the dynamics of long liquid bridges*, already used in

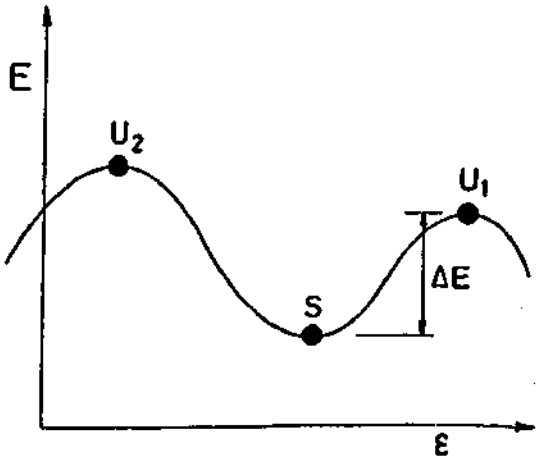

Fig. 5. Typical energy diagram for a long liquid bridge. In this plot E stands for the liquid bridge energy whereas ε is a parameter measuring, for instance, the magnitude of the deformation of the interface. Point S represents the stable configuration whereas U_1 and U_2 represent the unstable ones.

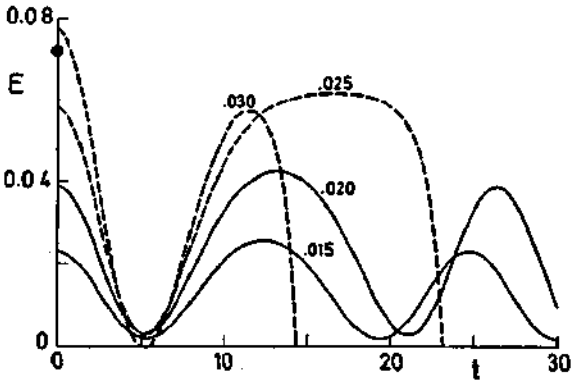

Fig. 6. Variation with the dimensionless time, t, of the dimensionless surface energy, E, defined as indicated in the text, of liquid bridges with $\Lambda=2.85$, $V=1.3$, $K=0.805$ and $B=0$. The dot line indicates the static stability margin for such liquid bridge configuration. Numbers on the curves indicate the magnitude of the initial perturbation, B_i.

* As demonstrated in Ref. 8, in the case of long, inviscid liquid bridges the radial momentum equation can be neglected. In this case the equations governing the dynamics of the liquid bridge are the continuity equation, $S_t+Q_z=0$ and the axial momentum equation, $Q_t+(Q^2/S)_z=-SP_z$, where $P=4[2S+(S_z)^2-SS_{zz}][4S+(S_z)^2]^{-3/2}+Bz$, with the appropriate initial and boundary conditions: $S(z,0)=S_i(z)$, $Q(z,0)=0$, $S(\pm\Lambda,t)=(1\pm h)^2$, $Q(\pm\Lambda,t)=0$, where $h=(1-K)/(1+K)$. In these expressions $S=F^2$ and $Q=F^2W$, where F stand for the equation of the interface shape and W for the axial velocity field. To write down the above formulation all magnitudes have been made dimensionless by using R_0 as characteristic lenght and $(\rho_w R_0^3/\sigma)^{1/2}$ as characteristic time. Additional details on this model can be found in Refs. 8, 9 and 11.

liquid bridge problems [8,9,17,18]. In the same plot the stability margin corresponding to the liquid bridge under consideration has been represented. As it can be observed, the liquid bridge evolutions whose initial excess of energy is higher than the stability margin end in a liquid column breakage, whereas oscillations appear when the excess of energy is small enough with respect to the stability margin. The static stability margin has been defined as the difference in energies between the closest unstable shape and the stable one; however, in dynamic processes, like the ones shown in Fig. 6, the real stability margin depends not only on the static stability margin but also on the nature of the initial perturbation. This is why a liquid bridge can break even if the imposed initial perturbation be smaller than the corresponding static stability margin, as it happens with the case $B_i = 0.025$ in Fig. 6. Of course the different evolutions shown in Fig. 6 are only an approximation of the real evolutions: they have been calculated by using an inviscid one-dimensional model (therefore no dissipative effects are acounted for) in which it is assumed that the effects due to the surrounding medium are negligible. However, both viscosity and a surrounding liquid of almost the same density than that of the liquid bridge increase the stability margin. The effect of the liquid viscosity is clear, and no additional explanations are needed. Concerning the surrounding liquid, there are, according to Ref. 9, two effects to be taken into account at least. The first effect is that the outer bath force the movements to be slower: a given excess of energy at $t = 0$ has to be spent not only in the movement of the liquid bridge but also in the movement of the outer liquid. In fact, the following relationship between the breaking time of a liquid bridge with an outer liquid, T_b, to the breaking time of a liquid bridge with no outer liquid, T_0, was calculated in Ref. 9.

$$T_b/T_o[1 + (\varrho_o/\varrho w) / (D^2 - 1)]^{1/2} \qquad (1)$$

This expression was one of the results of a linear analysis of the dynamics of liquid bridges; ϱ_o and ϱ_w stand for the density of the outer liquid and liquid bridge, respectively, and D is a dimensionless parameter that measures the size of the reservoir containing both liquid bridge and outer bath (in such analysis it is assumed that the reservoir is of circular cross-section, its radius being DR_0).

On the other hand, since the excess of initial energy has to be spent in the movement not only of the liquid bridge but also that of the outer liquid, the kinetic energy per unit of mass will be smaller and, in consequence, it could be that a stable liquid bridge, that could become unstable for a given perturbation if no outer liquid is considered, remains stable for the same perturbation when it is surrounded by another liquid. To have an idea of the order of magnitude of this effect, an estimation similar to that reported in Ref. 9 can be done: the energy needed by the liquid bridge will be proportional to its mass, $\varrho_w LR_0^2$, and to the square of some characteristic velocity, W, in the same way the outer liquid will need an energy proportional to its mass, $\varrho_o LR_0^2(D^2 - 1)$, and to the square of its characteristic velocity, $W/(D^2 - 1)$. Hence, from this very simplified reasoning can be deduced that the fraction of the total available energy spent in the liquid birdge is $[1 + (\varrho_o/\varrho_w)/(D^2 - 1)]^{-1}$, which is smaller than the energy that would correspond to the liquid bridge considered alone. It must be pointed out that, because of the outer liquid, the energy of the initial perturbation needed to reach a given stability margin level must be higher when an outer liquid exists than when the density of the outer medium is negligible. Thus, the outer liquid can be a stabilizing effect from the point of view of the dynamics.

EXPERIMENTAL RESULTS AND CONCLUSIONS

Experimental results are summarized in Fig. 7, where the symbols represent the liquid bridge configurations that were tested in the drop tower of INTA. White symbols indicate that during the free-falling period the liquid bridge interface oscillated whereas black ones indicate that the breakage of the liquid column took place. The shape of the symbols indicate the value of the Bond number before dropping, B_i; a circle means $0.01 \le B_i < 0.02$ and a square $0.02 \le B_i < 0.03$. Solid lines indicate the theorical stability limits ($K = 0.805$) corresponding to the values of the Bond number indicated. As it can be observed, experimental results are in agreement ith theoretical predictions: once Bond number is set to zero a liquid bridge will break if it is in the unstable region (with respect to the stability limit corresponding to $B = 0$) or oscillate if the fluid configuration lies in the stable region.

Concerning the evolutions in which the interface oscillates, little more can be said about: the free-fall period was too short with respect to the period of the oscillation, so that precise measurement of the natural frequencies or damping coefficients becomes im-

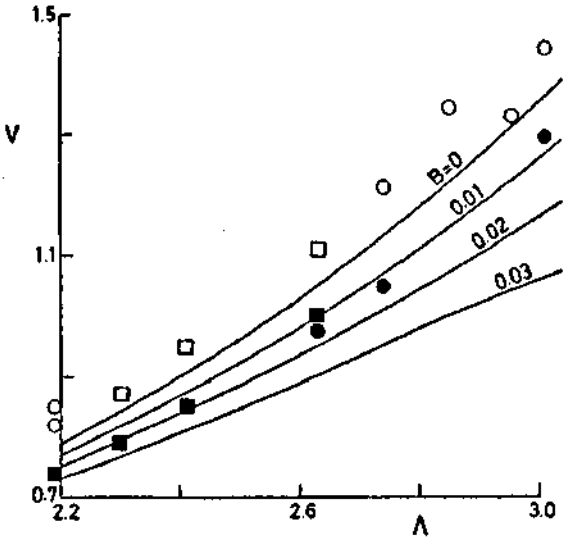

Fig. 7. Stability of liquid bridges between unequal disks ($K = 0.805$). Solid lines represent theoretical stability limits corresponding to the indicated values of Bond number, B, whereas the symbols represent experimental results. A black (white) symbol indicates that the brekaing (oscillation) of the liquid column took place after dropping. The shape of the symbols indicate the value of Bond number before dropping, B_i, a circle means $0.01 \le B_i < 0.02$ and a square $0.02 \le B_i < 0.03$.

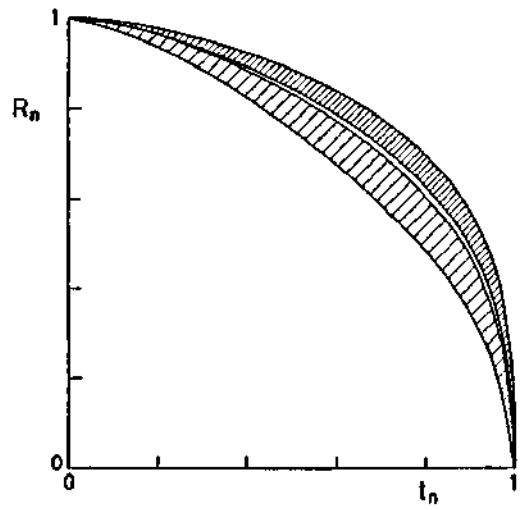

Fig. 8. Variation with the normalized time, t_n (defined as in the text) of the normalized radius, R_n, of the liquid bridge at section $z = -\Lambda/4$. The upper band corresponds to numerical results whereas the lower one corresponds to experimental results.

possible (to measure these characteristics of the liquid bridge dynamics the characteristic length, R_0, thus the characteristic time, would have been smaller to get several oscillations during the free-fall period, but then breaking processes would have been measured worse).

The evolutions in which a liquid column breakage took place are listed in Table 1, where experimental breaking times are compared with those resulting from numerical integration of the ODIS model (to write down dimensional values resulting from computations the characteristic time $t_c = 0.072$ s, already calculated in Section 2, has been used). Experimental breaking times are almost twice the calculated ones. This high difference could be partially explained by taking into account some peculiarities of the mathematical model involved. In effect, according to Ref. 11, the ODIS model gives breaking times some 10% smaller than those calculated by using a velocity-potential model which accounts for radial momentum effects. On the other hand, no outer liquid has been considered in calculations. As above stated, the presence of an outer liquid increases the brekaing time by an amount that depends on the density ratio ϱ_o/ϱ_w and on the distance D between the walls of the Plateau cell and the liquid bridge axis. Then, assuming that both liquids, outer bath and liquid bridge, are of the same density and taking $D \approx 3$, equation (1) gives $T_b/T_o \approx 1.06$. However, these two factors are not enough to explain the large discrepancies between theory and experiments concerning breaking time and it can be concluded that the ODIS model is only a rough tool when this aspect of the dynamics of liquid bridges is considered (in spite of that, other characteristics of the breaking process are accurately predicted by the ODIS model, this is the case of the volume of each one of the two main drops appearing after breakage [18]). To compare both numerical and experimental breaking evolutions the normalized breaking evolutions are shown in Fig. 8. In this plot the variation with normalized time, t_n (the time, t, divided by the breaking time, t_b: $t_n = t/t_b$) of the normalized radius at $z = -\Lambda/4$, R_n (the radius divided by the initial radius: $R_n = R(-\Lambda/4,t)/R(-\Lambda/4,0)$) has been represented. The lower band represents the envelope of all the experimental evolutions whereas the upper band includes all the numerical evolutions for the same values of Λ, V, K and B_i, calculated by using the ODIS model. Note that this numerical model gives sharp motions when compared with experimental results, the rate of change of the radius is slow at the beginning of the movement and afterwards suddenly accelerates.

The stability limits of liquid bridges between unequal disks, $K \neq 1$, have been experimentally analyzed by using a dynamic process in which an important characteristic of the stability diagram has been used (a liquid bridge between unequal disks can be more stable when an axial acceleration acts on the liquid column than when such an acceleration is removed). Experiments have been performed at the drop tower facility existing at INTA. The experimental procedure used to perform the experiments here described gives accurate knowledge of experimental initial conditions, otherwise almost impossible to be known when other experimental techniques commonly used in earth laboratories are employed, which could be used to experimentally check the validity of theoretical models to predict the non-linear behaviour of liquid bridges.

Table 1

Experimental and numerical breaking time, t_{be} and t_{bn}, respectively of liquid bridges between unequal disks

Λ	V	B_i	$t_{be}[s]$	$t_{bn}[s]$
2.19	0.741	0.024	1.02	0.529
2.30	0.789	0.023	1.16	0.554
2.41	0.858	0.030	1.09	0.605
2.63	0.971	0.016	1.29	0.663
2.63	0.994	>0.030	1.12	0.682
2.74	1.050	0.015	1.63	0.734
3.01	1.290	0.016	1.76	0.907

Acknowledgements—This work has been supported by the Spanish Comisión Interministerial de Ciencia y Tecnología (CICYT Project No. ESP92-0001-CP) and INTA.

REFERENCES

1. R. D. Gillette, R. C. Dyson, *Stability of fluid interfaces of revolution between equal solid circular plates*, Chem. Eng. J. 2, p. 44-54 (1971).
2. I. Da Riva, I. Martínez, *Floating zone stability* (Exp. 1-ES-331). ESA SP-142, p. 67-73 (1979).
3. I. Martínez, *Stability of axisymmetric liquid bridges*. ESA SP-191, p. 267-273 (1983).
4. S. R. Coriell, S. C. Hardy, M. R. Cordes, *Stability of Liquid Zones*. J. Colloid Interface Sci. 60, p. 126-136 (1977).
5. L. Slobozhanin, J. M. Perales, *Stability of liquid bridges between equal disks in an axial gravity field*. Phys. Fluid A 5, p. 1305-1314 (1993).
6. J. Meseguer, *Stability of slender, axisymmetric liquid bridges between unequal disks*. J. Crystal Growth 67, p. 141-143 (1984).

7. J. M. Perales, J. Meseguer, I. Martínez, *Minimum volume stability limits for axisymmetric liquid bridges subject to steady axial acceleration*. J. Crystal Growth **110**, p. 855-861 (1991).
8. J. Meseguer, *The breaking of axisymmetric slender liquid bridges*. J. Fluid Mech. **130**, p. 123-151 (1983).
9. A. Sanz, *The influence of the outer bath on the dynamics of axisymmetric liquid bridges*. J. Fluid Mech. **156**, p. 101-140 (1985).
10. Y. Zhang, J. I. D. Alexander, *Sensitivity of liquid bridges subject to axial residual acceleration*. Phys. Fluids A **2**, p. 1966 (1990).
11. R. M. S. M. Schulkes, *Non-linear dynamics of liquid columns: A comparative study*. Phys. Fluids A **5**, p. 2121-2130 (1993).
12. N. Bezdenejnykh, J. Meseguer, J. M. Perales, *Experimental analysis of stability limits of capillary liquid bridges*. Phys. Fluids A. **4**, p. 677-680 (1992).
13. A. Sanz, I. Martínez, *Minimum volume for a liquid bridge between equal disks*. J. Colloid Interface Sci. **93**, p. 235-240 (1983).
14. J. Meseguer, L. A. Mayo, J. C. Llorente, A. Fernández, *Experiments with liquid bridges in simulated microgravity*. J. Crystal Growth **73**, p. 609-621 (1985).
15. J. Meseguer, A. Sanz, J. López, *Liquid bridge breakages aboard Spacelab-D1*. J. Crystal Growth **78**, p. 325-334 (1986).
16. I. Martínez, A. Sanz, *Experiments with long liquid columns under microgravity*, ESA SP-295, p. 413-419 (1990).
17. J. Meseguer, A. Sanz, *Numerical and experimental study of the dynamics of axisymmetric liquid bridges*. J. Fluid Mech. **153**, p. 83-101 (1985).
18. J. Meseguer, J. M. Perales, N. Bezdenejnykh, *A theoretical approach to impulsive motion of viscous liquid bridges*. Microgravity Q., Vol. 1, No. 4, p. 215-219 (1991).
19. C. Bisch, A. Lasek, H. Rodot, *Comportement hydrodynamique de volumes liquides spheriques semi-libres en apesanteur simuleé*. Journal de Méchanique Théorique et Appliquée **1**, p. 165-183 (1982).